Supporting Information

Enhancing Activity and Stability of RuO_2 as Bifunctional Catalyst Using Thermally Tuned α-MnO_2 Interlayer for Hydrogen Production

Shashwat Bishwanathan[1], Simran Kaur Oberoi[1], Maurya Gyanprakash[2], Prashant Kumar Gupta[1],*

[1]Department of Chemical Engineering, Indian Institute of Technology Jodhpur, Jodhpur Rajasthan-342030, India.

[2]Centre for Advanced Studies, AKTU, Jankipuram, Lucknow, Uttar Pradesh-226031, India

* Corresponding author: guptapk@iitj.ac.in

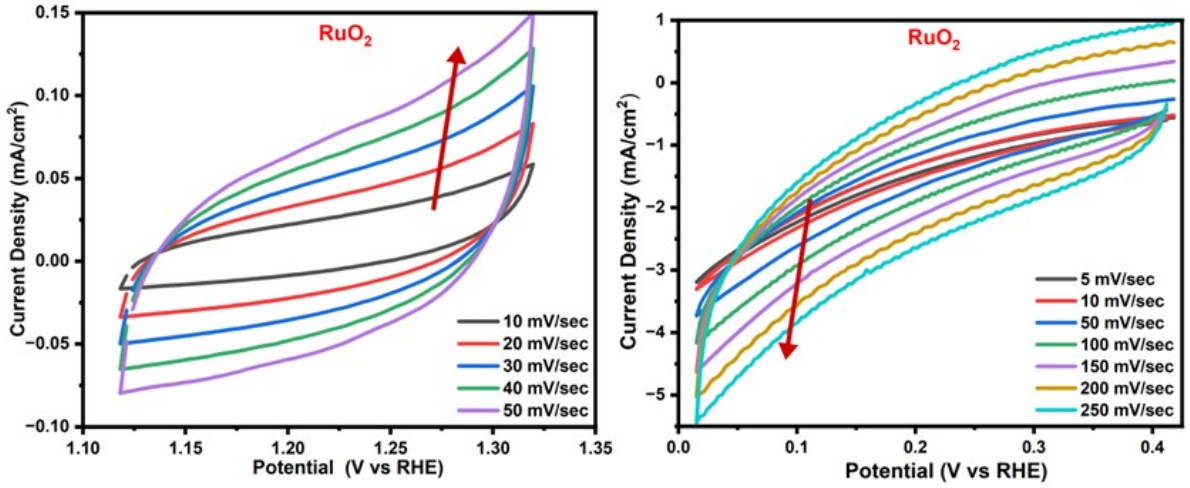

Figure S1: Cyclic Voltammetry of RuO_2 at different scan rates in the non-faradaic region for the calculation of C_{dl} and ECSA (a) In OER at a scan rate of 10, 20, 30, 40, and 50 mV/sec, (b) In HER at a scan rate of 5, 10, 50, 100, 150, 200, and 250 mV/sec

Double layer capacitance (C_{dl}) and Electrochemical Active sites (ECSA) Calculation:

1. **Double Layer Capacitance (C_{dl})**: The C_{dl} value is determined using the CV technique in the non-faradaic area. It is computed using the formula: $I = C_{dl} \times \nu$, where ν represents the sweep rate (mV/sec). The sweep rate ranges from 10-50 mV/sec for OER and 5-250 mV/sec for HER, as shown in Figure.

   The current value is taken at 1.20 V vs. RHE for OER and 0.2 V vs. RHE for HER, and the slope of the I v/s ν is double-layer capacitance (C_{dl}) for the corresponding electrodes.
2. **Electrochemical Active Surface Area (ECSA):** ECSA is calculated from the formula:

$$ECSA = C_{dl}/C_s,$$

$C_s = 40\ \mu F/cm^2$ because of the planar geometry of the electrode and alkaline environment[1]

Substrate Pretreatment Procedure:

Carbon Paper – Carbon paper measuring 2×1 cm^2 was ultrasonicated in acetone for 60 minutes at a temperature of 50 °C, followed by cleaning with MilliQ water to eliminate the acetone and any extraneous substances. Subsequently, it undergoes a drying process for 3 hours at a temperature of 60 °C.

Nickel Foam- The nickel foam of identical dimensions was subjected to treatment with 3 M HCl, ethanol, acetone, and MilliQ water, each for a duration of 15 minutes. Subsequently, it undergoes a drying process in a vacuum oven for a duration of 12 hours.

Ink Preparation: After synthesizing α-MnO_2 in powdered form, the ink for drop casting was created by dispersing 5 mg of catalyst particles in 5 mL of isopropanol. In addition, the binder Nafion 117, with a weight of 20 µL (5% by weight), was used. To prepare the RuO_2 ink, we combined 5 mg of heat-treated

RuO_2 with 5 mg of acetylene black. These were then dispersed in a combination of 90 µL Nafion 117 and 700 µL of a 1:1 ratio mixture of IPA and water. The mixture is sonicated for 1 hour before drop-casting. The ink for 20 wt% Pt/C was prepared using 5 mg of Pt/C added into 90 µL Nafion 117 and 700 µL of a 1:1 ratio mixture of IPA and water.

Membrane Preconditioning: The membrane is preconditioned by being kept in a 0.5 M NaCl solution for 24 hours at room temperature, then followed by storage in a 1 M KOH solution for an additional 24 hours at room temperature. Prior to use in the H cell electrolyzer, the membrane was cleaned many times with MilliQ water.

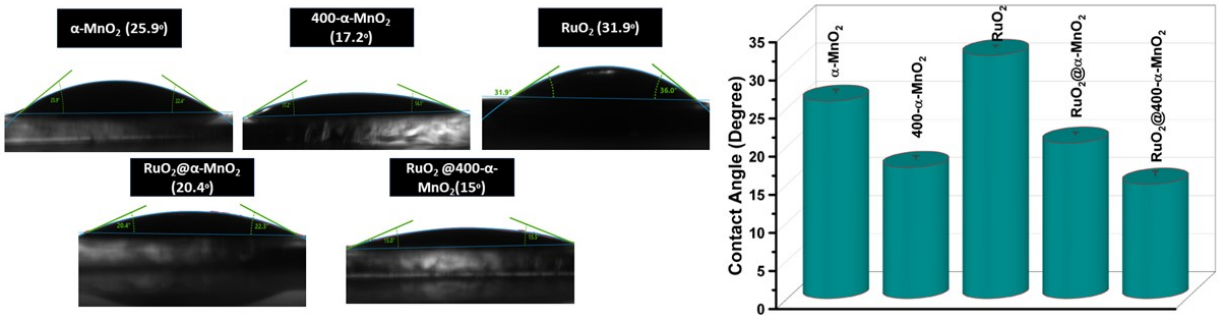

Figure S2: Contact angle measurement

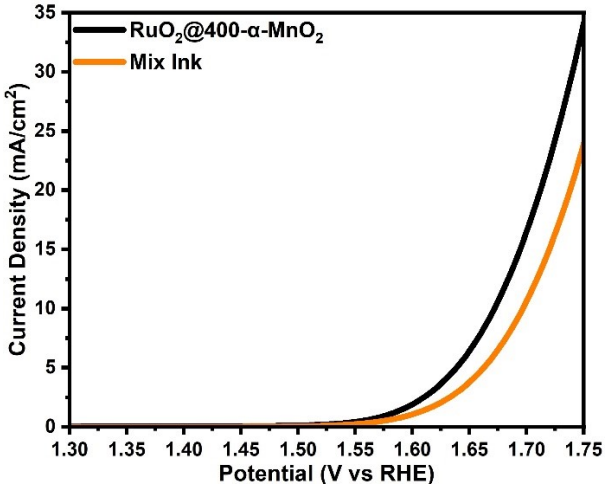

Figure S3: LSV comparison of RuO_2@400-α-MnO_2 and electrode prepared with mixing ink in the same composition of 400-α-MnO_2 and RuO_2

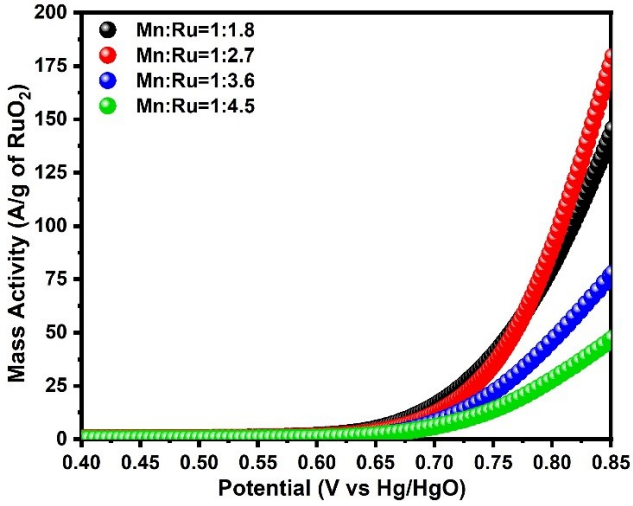

Figure S4: LSV comparison for the different mass ratios of 400-α-MnO_2 and RuO_2 for preparing electrode of RuO_2@400-α-MnO_2

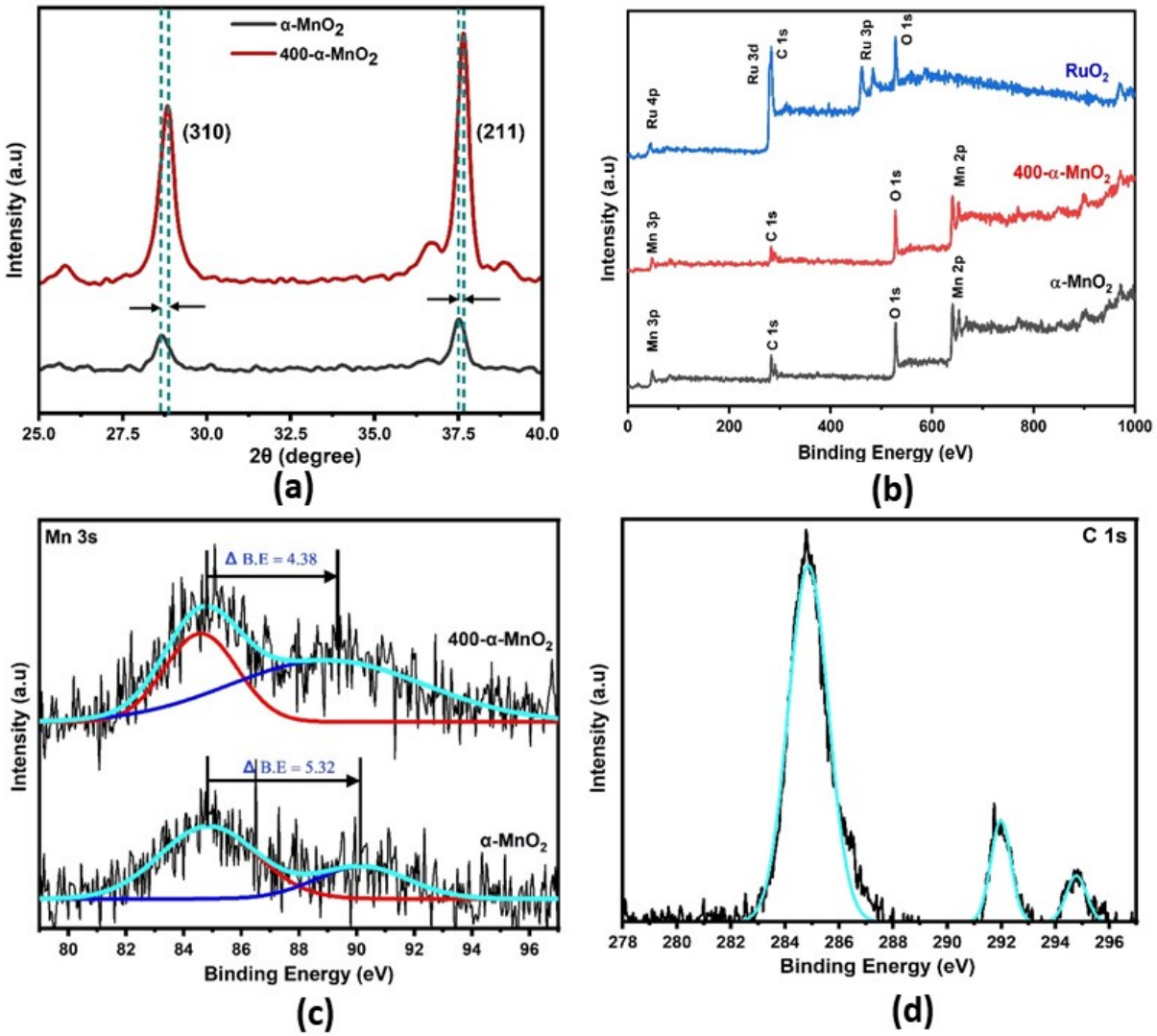

Figure S5: (a) Magnified XRD peaks for (310) and (211) displacement, (b) Fast scan survey spectra, (c) XPS scan Mn 3s for α-MnO_2 and 400-α-MnO_2, (d) C 1s XPS scan for calibration

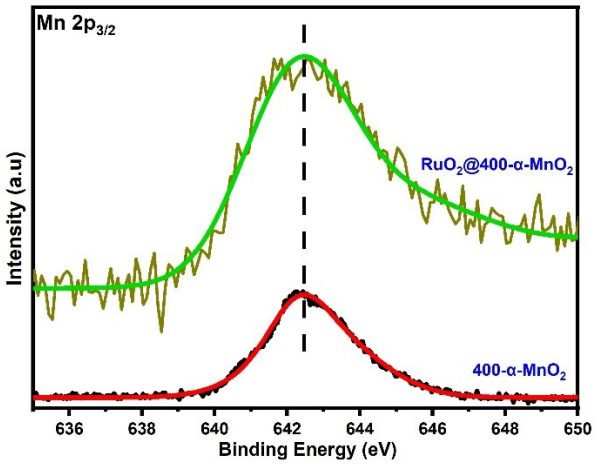

Figure S6: XPS spectra for Mn $2p_{3/2}$ for 400-α-MnO_2 and RuO_2@400-α-MnO_2

	Average Crystallite Size (nm)$	d-spacing for (310) plane (Å)	d-spacing for (211) plane (Å)	Lattice Constants (Å)	Cell Volume (Å^3)
α-MnO_2	14.66	3.1097	2.3949	a=b=9.83; c=2.856	275.96
400- α-MnO_2	14.16	3.0959	2.3876	a=b=9.79; c=2.848	273.25

Table S1: XRD outputs for α-MnO_2 and 400-α-MnO_2

$ - Nanocrystallite size calculated with Scherrer equation

	α-MnO_2	400-α-MnO_2	RuO_2	RuO_2@α-MnO_2	RuO_2@400-α-MnO_2
Resistivity (Ω/cm)	0.61	0.53	0.81	1.03	0.54
Conductivity (S-cm)	1.64	1.88	1.24	0.97	1.83

Table S2: Resistivity and conductivity data obtained from Four probe Hall measurement instrument

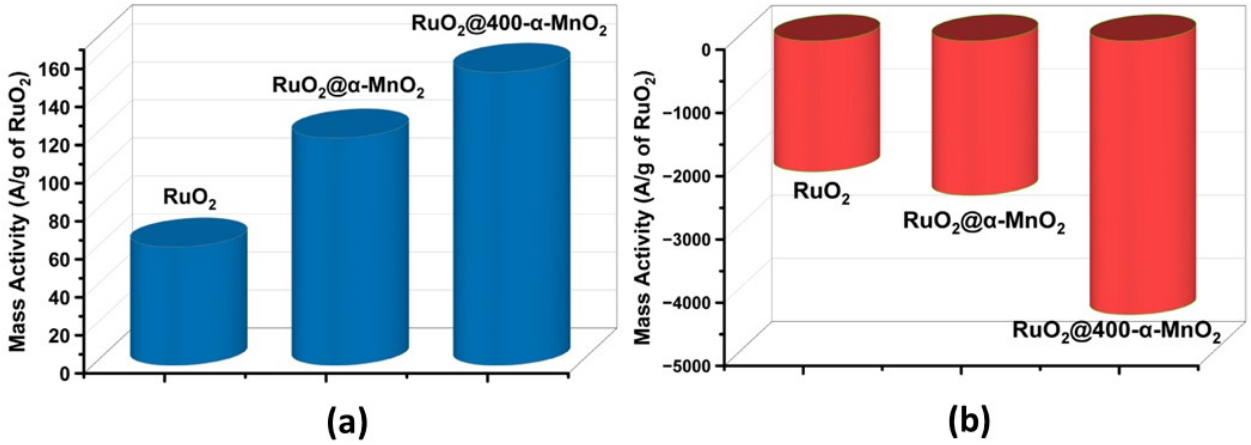

Figure S7: Mass Activity plots; (a) OER at an overpotential of 500 mV, (b) HER at an overpotential of 350 mV

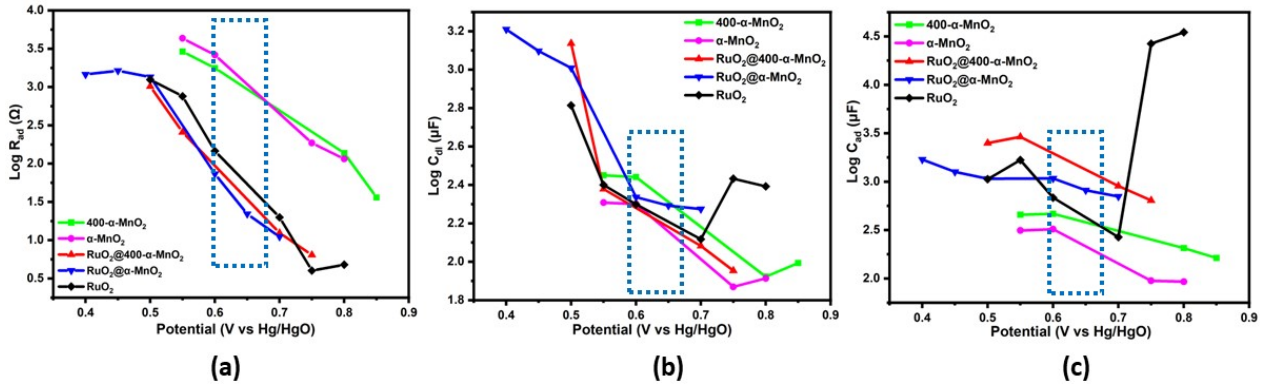

Figure S8: (a) Logarithmic of Adsorption Resistance, (b) Double Layer capacitance, and (c) Adsorption Capacitance Variation with Potential for OER Electrocatalysts. The blue dashed area shows the onset region for different samples.

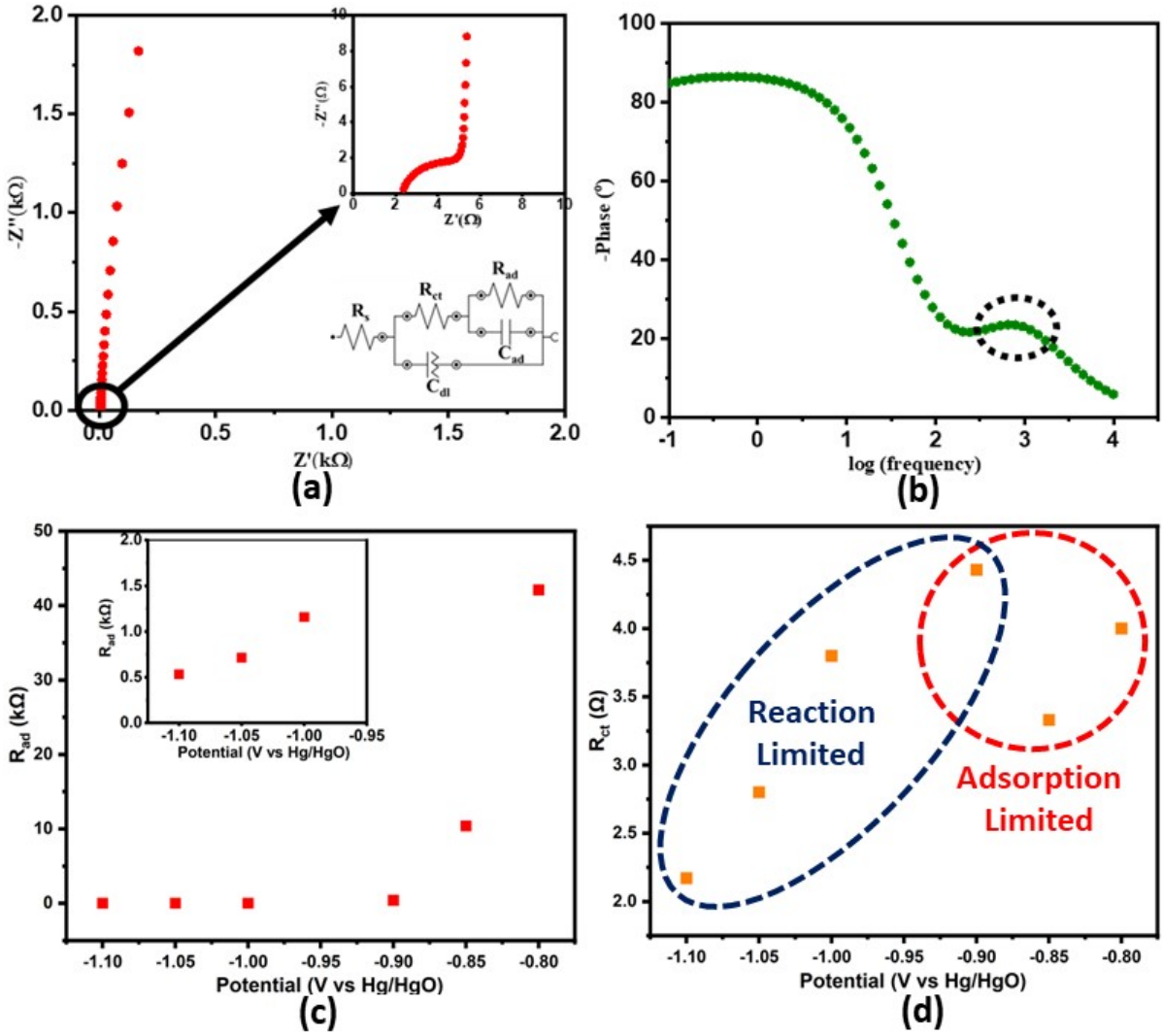

Figure S9: (a) Nyquist plot at OCP obtained from EIS; inset represents the corresponding fitted circuit (b) Bode plot; variation of (c) Adsorption resistance and (d) Charge transfer resistance with potential

	C_{dl} at 0.5 V for OER	C_{dl} at -0.85 V for HER
RuO_2	651 μF	4.14 mF
RuO_2@α-MnO_2	1020 μF	5.59 mF
RuO_2@400-α-MnO_2	1370 μF	12.4 mF

Table S3: Double Layer Capacitance (C_{dl}) calculated from EIS study. The potential value is taken in non-Faradaic regions and v/s Hg/HgO

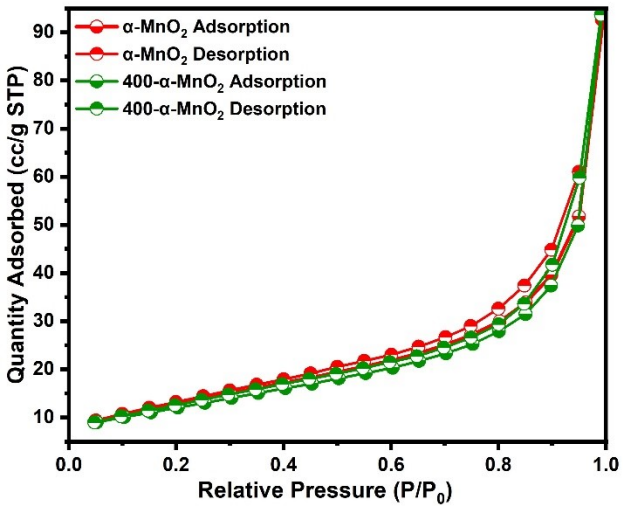

Figure S10: Nitrogen adsorption-desorption isotherm

	MBET Surface Area*	Langmuir Surface Area&	BJH Surface Area%	BJH Pore Volume
MnO_2	47.178 m^2/g	75.115 m^2/g	28.88 m^2/g	0.133 cc/g
400-MnO_2	43.712 m^2/g	69.78 m^2/g	27.08 m^2/g	0.136 cc/g

Tabel S4: BET surface areas and Pore volume

*- BET surface area through multi-point data

&- BET surface area through Langmuir

% - BET Surface area through Barret-Joyner-Halenda (BJH) Method

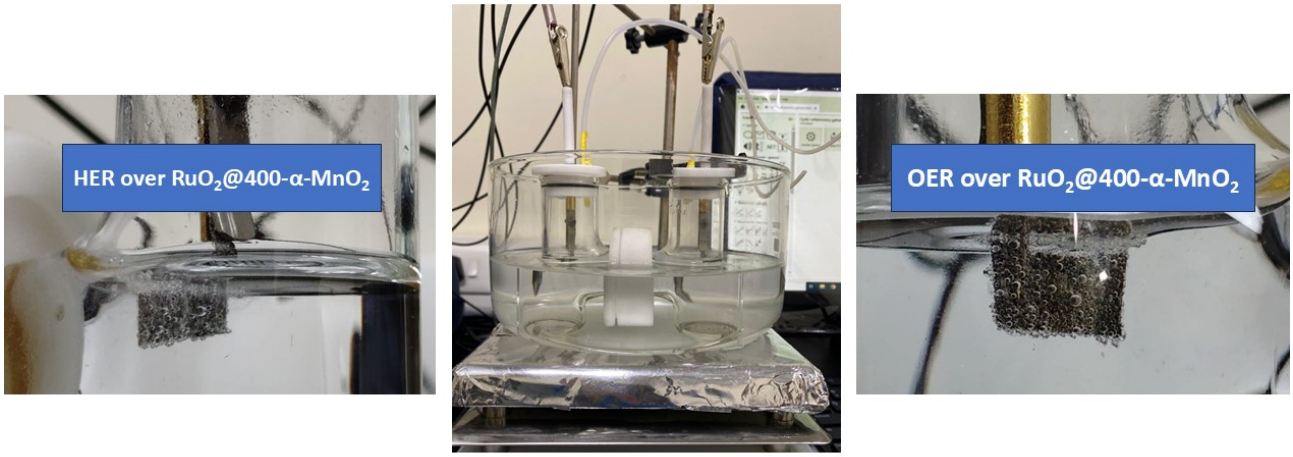

(a) (b) (c)

Figure S11: AEM membrane-based H-Cell setup for full-cell performance test; (a) Hydrogen bubbling over RuO_2@400-α-MnO_2 at the cathode, (b) H-Cell setup, (c) Hydrogen bubbling over RuO_2@400-α-MnO_2 at the anode

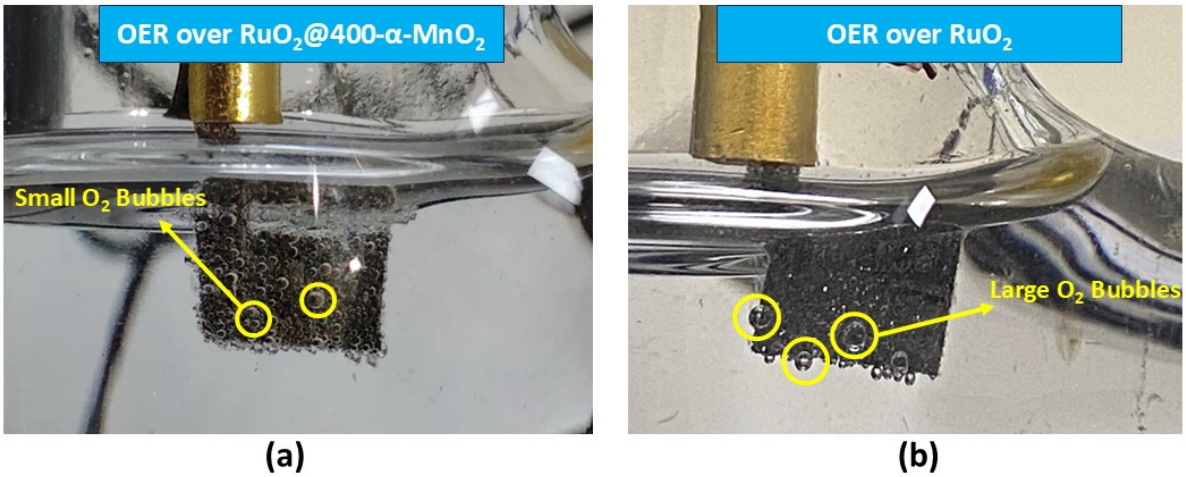

Figure S12: (a) Fast bubble release from the RuO_2@400-α-MnO_2 surface, (b) Large bubble formation over RuO_2 surface

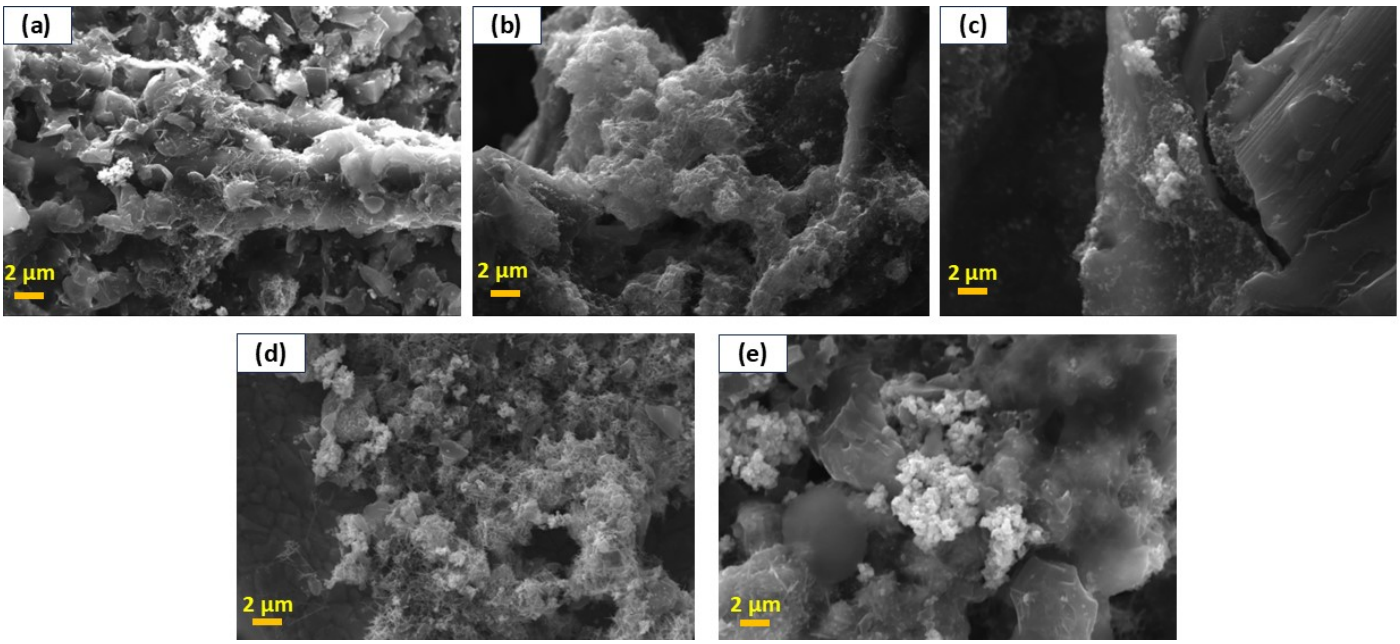

Figure S13: Pre and Post stability test SEM images of RuO_2@400-α-MnO_2 electrode at a magnification of 2 µm, (a) Fresh RuO_2@400-α-MnO_2@carbon paper, (b) RuO_2@400-α-MnO_2@carbon paper after 20 hours OER stability test, (c) RuO_2@400-α-MnO_2@carbon paper after 20 hours HER stability test, (d) RuO_2@400-α-MnO_2@Nickel Foam after 40 hours OER stability test, (e) RuO_2@400-α-MnO_2@Nickel Foam after 40 hours HER stability test

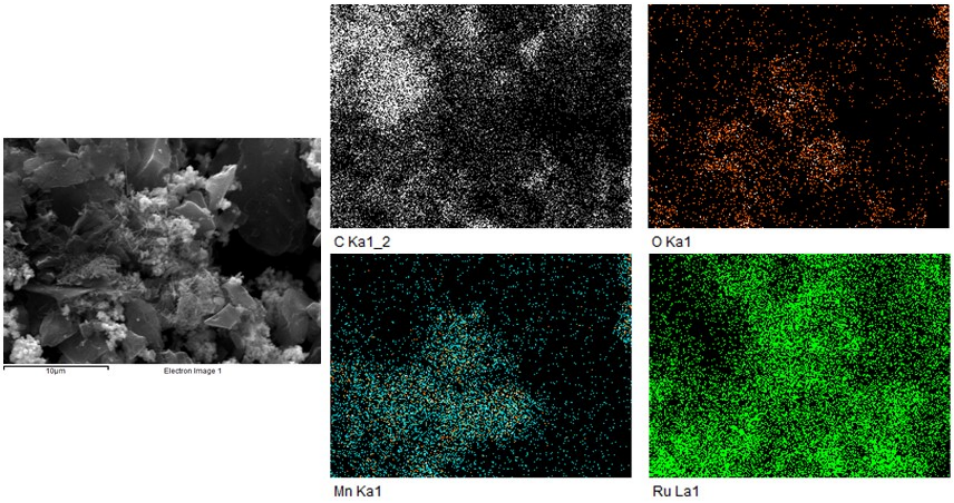

Figure S14: Pre-stability elemental mapping for RuO_2@400-α-MnO_2

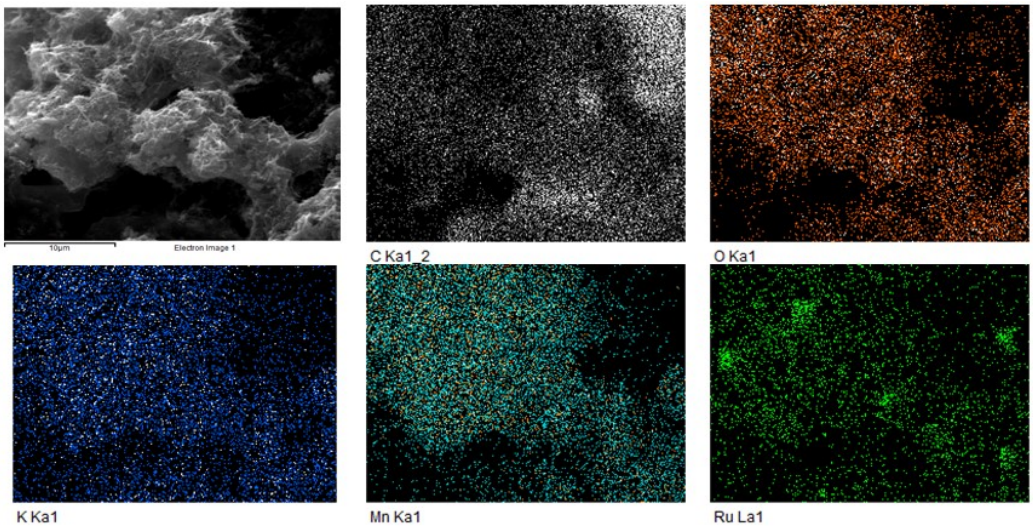

Figure S15: Elemental mapping image for RuO_2@400-α-MnO_2@carbon paper after 20 hours OER stability test

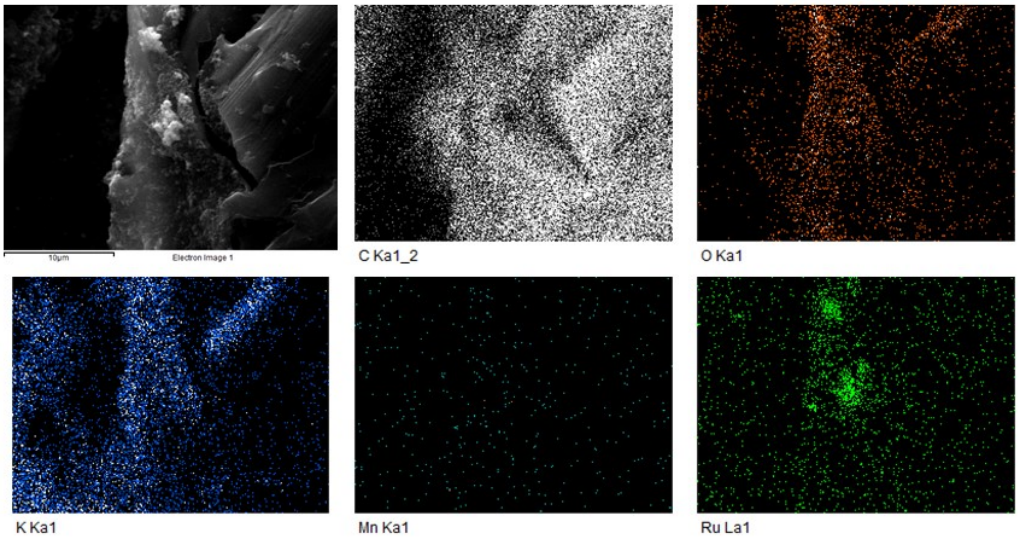

Figure S16: Elemental mapping image for RuO_2@400-α-MnO_2@carbon paper after 20 hours HER stability test

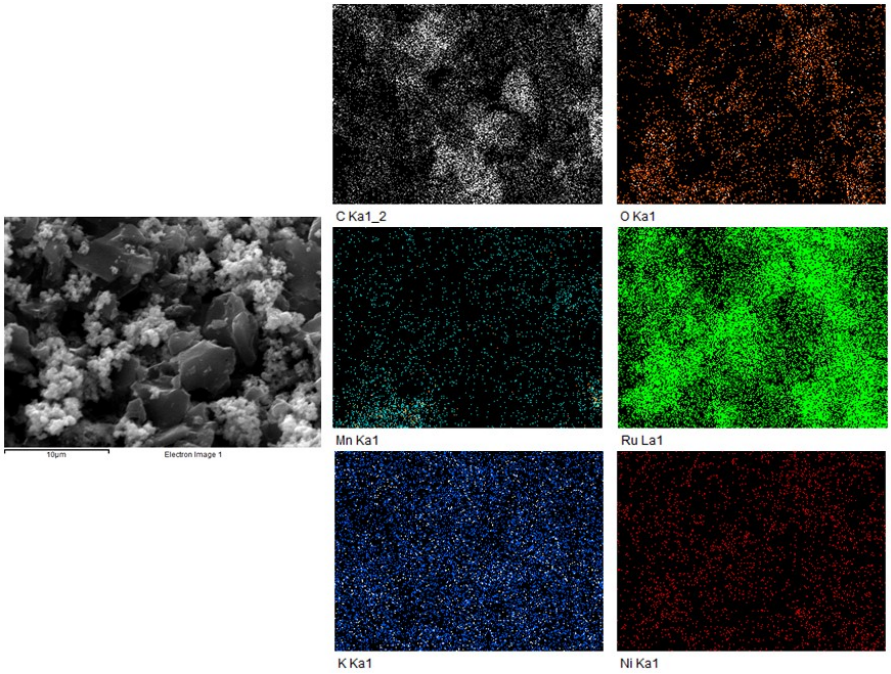

Figure S17: Elemental mapping image for RuO_2@400-α-MnO_2@Nickel Foam after 40 hours OER stability test

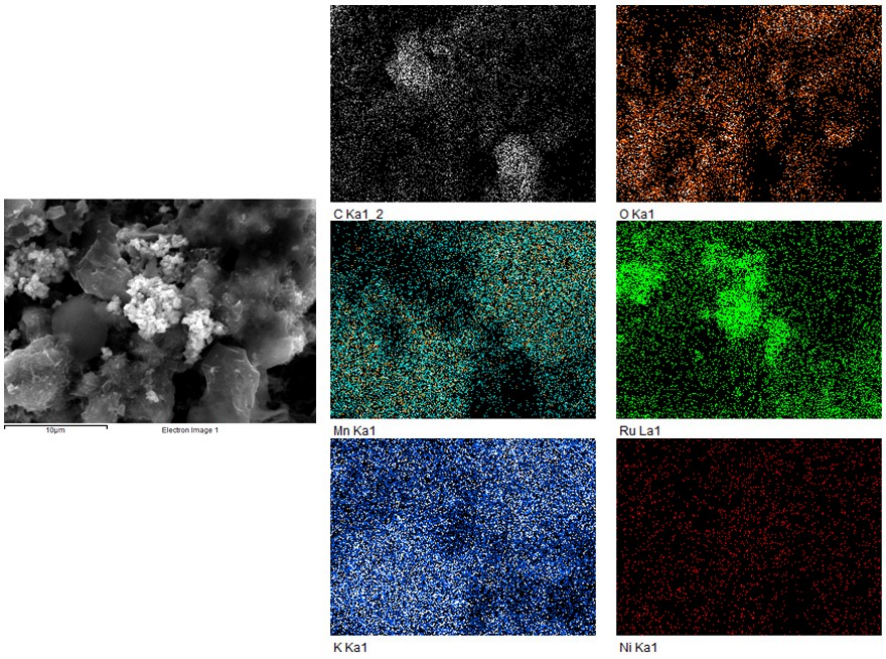

Figure S18: Elemental mapping image for RuO_2@400-α-MnO_2@Nickel Foam after 40 hours HER stability test

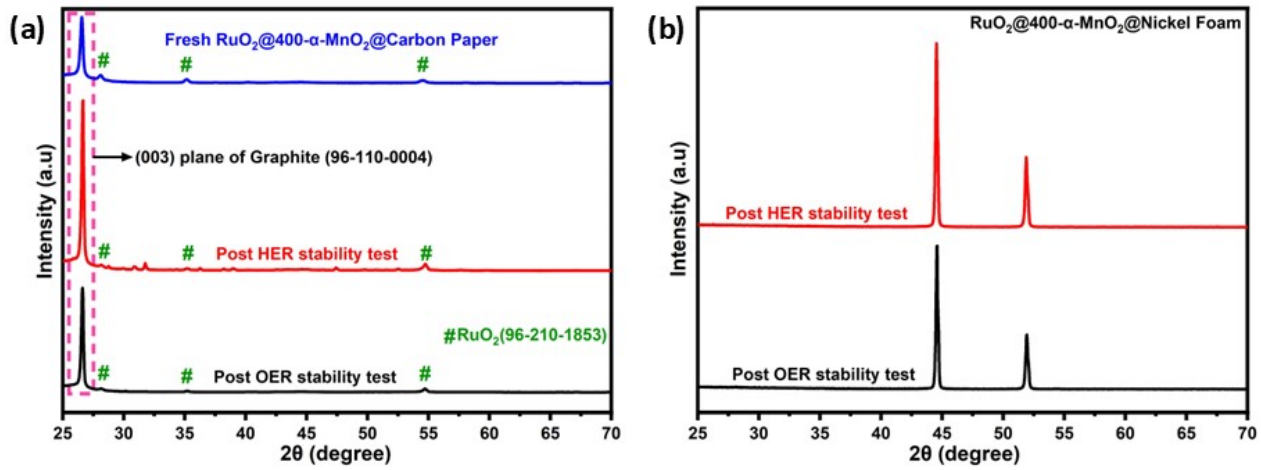

Figure S19: X-ray Diffraction pattern for (a) RuO_2@400-α-MnO_2@Carbon Paper pre and post-20 hours stability test used for half-cell study, (b) RuO_2@400-α-MnO_2@Nickel Foam after 40 hours of stability test used in the full-cell study

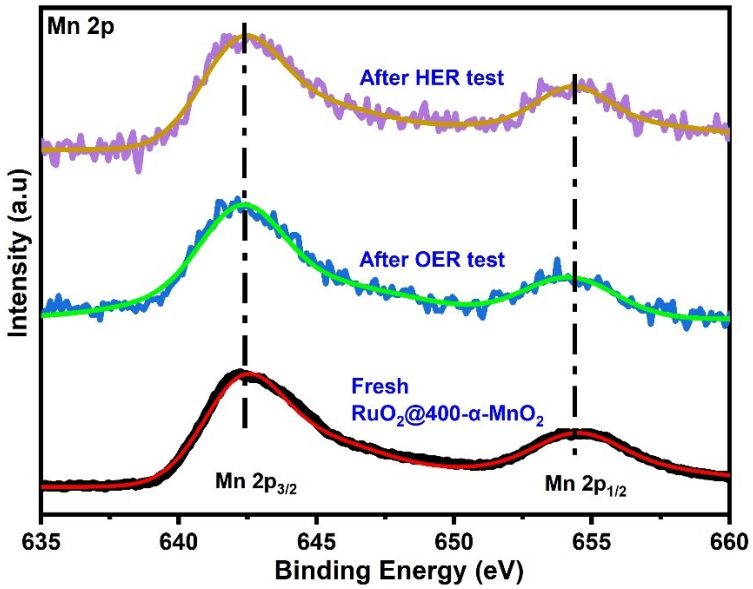

Figure S20: XPS spectra of Mn 2p for fresh RuO_2@400-α-MnO_2 and after OER, HER stability test

Catalyst	Loading (mg/cm^2)	OER Tafel	HER Tafel	Cell Voltage @ 10 mA/cm^2	Stability (hours)	Membrane
This Study	**0.189**	**63.5**	**24.5**	**1.485**	**40**	**AEM**
RuO_2@NiO[2]	0.2	50.5	31.7	1.5	12	without
RuO_2@Co_3O_4[3]	0.285	69	91	1.645	1000 cycle	without
Ru aerogel[4]	1	81	35	1.46	14	without
Ru/RuO_2@MoO_2 [5]	0.416	65	50	1.54	40	with
Ni@Ru[6]	0.35-0.40	89.6	87.3	1.61	--	without
$NiRuO_{2-x}$[7]	--	66	34.4	1.6	20	with
Ru/Cu-doped RuO_2[8]	0.285	56	35	1.47	11	with
CoO_x-RuO_2[9]	--	69.6	42.1	1.49	48	without

Table S5: Comparison of RuO_2-based bifunctional electrocatalytic performance in 1M KOH

REFERENCES:

1. McCrory, C.C.L., Jung, S., Peters, J.C., and Jaramillo, T.F. (2013) Benchmarking heterogeneous electrocatalysts for the oxygen evolution reaction. *J. Am. Chem. Soc.*, **135** (45), 16977–16987.
2. Liu, J., Zheng, Y., Jiao, Y., Wang, Z., Lu, Z., Vasileff, A., and Qiao, S.Z. (2018) NiO as a Bifunctional Promoter for RuO2 toward Superior Overall Water Splitting. *Small*, **14** (16), 1–10.
3. Liu, H., Xia, G., Zhang, R., Jiang, P., Chen, J., and Chen, Q. (2017) MOF-derived RuO2/Co3O4 heterojunctions as highly efficient bifunctional electrocatalysts for HER and OER in alkaline solutions. *RSC Adv.*, **7** (7), 3686–3694.
4. Yan, S., Liao, W., Zhong, M., Li, W., Wang, C., Pinna, N., Chen, W., and Lu, X. (2022) Partially oxidized ruthenium aerogel as highly active bifunctional electrocatalyst for overall water splitting in both alkaline and acidic media. *Appl. Catal. B Environ.*, **307** (February), 121199.
5. Fan, Y., Zhang, X., Zhang, Y., Xie, X., Ding, J., Cai, J., Li, B., Lv, H., Liu, L., Zhu, M., Zheng, X., Cai, Q., Liu, Y., and Lu, S. (2021) Decoration of Ru/RuO2 hybrid nanoparticles on MoO2 plane as bifunctional electrocatalyst for overall water splitting. *J. Colloid Interface Sci.*, **604**, 508–516.
6. Wu, W., Wu, Y., Zheng, D., Wang, K., and Tang, Z. (2019) Ni@Ru core-shell nanoparticles on flower-like carbon nanosheets for hydrogen evolution reaction at All-pH values, oxygen evolution reaction and overall water splitting in alkaline solution. *Electrochim. Acta*, **320**, 134568.
7. Chen, X., Song, J., Xing, Y., Qin, Y., Lin, J., Qu, X., Sun, B., Du, S., Shi, D., Chen, C., and Sun, D. (2023) Nickel-decorated RuO2 nanocrystals with rich oxygen vacancies for high-efficiency overall water splitting. *J. Colloid Interface Sci.*, **630** (1), 940–950.
8. Yang, K., Xu, P., Lin, Z., Yang, Y., Jiang, P., Wang, C., Liu, S., Gong, S., Hu, L., and Chen, Q. (2018) Ultrasmall Ru/Cu-doped RuO2 Complex Embedded in Amorphous Carbon Skeleton as Highly Active Bifunctional Electrocatalysts for Overall Water Splitting. *Small*, **14** (41), 1–10.
9. Yu, T., Xu, Q., Qian, G., Chen, J., Zhang, H., Luo, L., and Yin, S. (2020) Amorphous CoOx-Decorated Crystalline RuO2Nanosheets as Bifunctional Catalysts for Boosting Overall Water Splitting at Large Current Density. *ACS Sustain. Chem. Eng.*, **8** (47), 17520–17526.